Letter

# Pair correlations of the hybridized orbitals in a ladder model for the bilayer nickelate $La_3Ni_2O_7$

Masataka Kakoi,[1] Tatsuya Kaneko,[1] Hirofumi Sakakibara,[2] Masayuki Ochi,[1,3] and Kazuhiko Kuroki[1]
[1]*Department of Physics, Osaka University, Toyonaka, Osaka 560-0043, Japan*
[2]*Advanced Mechanical and Electronic System Research Center(AMES), Faculty of Engineering, Tottori University, Tottori, Tottori 680-8552, Japan*
[3]*Forefront Research Center, Osaka University, Toyonaka, Osaka 560-0043, Japan*

(Received 8 December 2023; revised 8 April 2024; accepted 8 May 2024; published 24 May 2024)

To clarify the nature of high-temperature superconductivity in the bilayer nickelate $La_3Ni_2O_7$ under pressure, we investigate, using the density-matrix renormalization group method, the pair correlations in the two-orbital $t$-$J$ ladder model. While the interchain-intraorbital pair correlations exhibit a slow power-law decay in both orbitals, the interorbital pair correlation also develops strongly enough to be comparable with the intraorbital correlations. These intra and interorbital pair correlations are enhanced by Hund's coupling, but more importantly, the interorbital pair correlation develops even when interorbital pairing glue mediated by Hund's coupling is absent. Our finding suggests that the pair correlation in the present system develops as a hybridized two-orbital entity, which may have some implications on the superconductivity in the bilayer nickelate.

DOI: 10.1103/PhysRevB.109.L201124

The recent discovery of high-temperature superconductivity under pressure with a $T_c$ of $\sim$80 K in a bilayer Ruddlesden-Popper nickelate $La_3Ni_2O_7$ [1] has initiated a new intensive wave of research in the field of condensed matter physics. Experimental reproductions that have followed the initial discovery have indeed established the occurrence of superconductivity in this material [2–7]. Also, already a large number of theoretical studies have appeared after the discovery of superconductivity [8–45]. Moreover, even the trilayer nickelate $La_4Ni_3O_{10}$ has been found to exhibit signatures of superconductivity under pressure with a lower $T_c$ of about 25 K [5,46–48], as expected theoretically [5].

Regarding the theories on $La_3Ni_2O_7$ that focus on the pairing mechanism, many of them agree on the point that the pairing involves interlayer nature, where the large interlayer hopping between the nearly half-filled $d_{3z^2-r^2}$ orbitals (or the interlayer magnetic exchange coupling induced by the interlayer hopping) plays an important role, which was a feature theoretically pointed out for this material in Ref. [49] by one of the present authors before the experimental discovery. In fact, a nearly half-filled Hubbard (or $t$-$J$) model on a bilayer lattice [49–53] or a two-leg ladder [54–56] has been known to be favorable for superconductivity for many years. However, in $La_3Ni_2O_7$, along with the nearly half-filled $d_{3z^2-r^2}$ orbitals, there exist nearly quarter-filled $d_{x^2-y^2}$ orbitals. The role played by the coupling between the $d_{3z^2-r^2}$ and $d_{x^2-y^2}$ orbitals, namely, the single-particle hybridization and the two-body interactions such as Hund's coupling, and also, which one of the two orbitals dominates in the pairing, have been issues of debate.

In Ref. [39], three of the present authors discussed the role played by those interorbital interactions using fluctuation exchange approximation, which is basically a weak coupling approach. On the other hand, we used the density-matrix renormalization group (DMRG) method [57–59] to study the interlayer pair correlations in a two-orbital two-leg Hubbard ladder that mimics the electronic structure of $La_3Ni_2O_7$ in a one-dimensional system (but without considering the interorbital two-body interactions) [40]. There it was found that orbitals corresponding to the $d_{3z^2-r^2}$ and $d_{x^2-y^2}$ orbitals both exhibit slowly decaying correlations, even without Hund's coupling, with the former somewhat dominating in the decaying power. DMRG has also been adopted to investigate different types of models of $La_3Ni_2O_7$ [41–45]. In terms of the two-orbital models, the numerical elucidation of the interplay of the $d_{3z^2-r^2}$ and $d_{x^2-y^2}$ orbitals is highly desired to approach the pairing mechanism in $La_3Ni_2O_7$.

Given this background, to further investigate the effect of the interorbital interactions, here we study the pair correlations using DMRG in a two-orbital $t$-$J$ ladder that mimics $La_3Ni_2O_7$ in a similar manner as in Ref. [40], not only including the interlayer exchange coupling explicitly, but also considering Hund's coupling. We find that Hund's coupling encourages the correlations of the interchain pairs of both nearly half-filled (i.e., $d_{3z^2-r^2}$) and nearly quarter-filled (i.e., $d_{x^2-y^2}$) orbitals. More importantly, our calculation demonstrates that the correlation of the interorbital pairs exhibits a slow power-law decay, and this decaying behavior appears even without Hund's coupling. Our finding suggests that the hybridized orbital due to interorbital hopping (that exists in actual $La_3Ni_2O_7$) obtains the quasi-long-range superconducting correlation.

To address the issues, we consider a two-orbital $t$-$J$ model [see Fig. 1], which is an effective model of the two-orbital Hubbard model in the strong coupling limit. Our $t$-$J$ model set in the ladder lattice prohibits the doubly occupied orbital at 3/8 filling, and the Hamiltonian $\hat{H} = \hat{H}_t + \hat{H}_J$ consists of

 

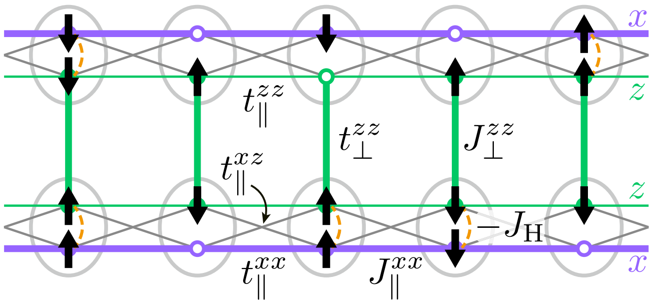


FIG. 1. Two-orbital $t$-$J$ ladder at 3/8 filling. The $x$ and $z$ orbitals correspond to the $d_{3z^2-r^2}$ and $d_{x^2-y^2}$ orbitals, respectively, in the bilayer nickelate.

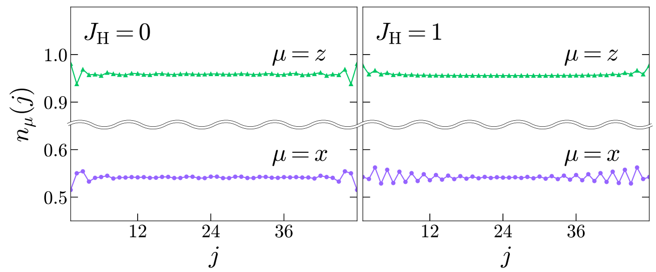


FIG. 2. Local electron density $n_\mu(j) = 1/2\sum_l \langle \hat{n}_{j,l,\mu}\rangle$ at $J_{\mathrm{H}} = 0$ (left panel) and $J_{\mathrm{H}} = 1$ (right panel), where $J_{\perp}^{zz} = 0.5$.

the one-body term

$$\hat{H}_t = -\sum_{\mu,\nu} t_{\parallel}^{\mu\nu} \sum_{j,l}\sum_{\sigma}(\hat{\tilde{c}}^{\dagger}_{j,l,\mu,\sigma}\hat{\tilde{c}}_{j+1,l,\nu,\sigma} + \mathrm{H.c.}) - t_{\perp}^{zz}\sum_{j}\sum_{\sigma}(\hat{\tilde{c}}^{\dagger}_{j,1,z,\sigma}\hat{\tilde{c}}_{j,2,z,\sigma} + \mathrm{H.c.}) + \frac{\Delta E}{2}\sum_{j,l}(\hat{n}_{j,l,x} - \hat{n}_{j,l,z}) \quad (1)$$

and the spin interaction term

$$\hat{H}_J = J_{\parallel}^{xx}\sum_{j,l}\left(\hat{\mathbf{S}}_{j,l,x}\cdot\hat{\mathbf{S}}_{j+1,l,x} - \frac{1}{4}\hat{n}_{j,l,x}\hat{n}_{j+1,l,x}\right) + J_{\perp}^{zz}\sum_{j}\left(\hat{\mathbf{S}}_{j,1,z}\cdot\hat{\mathbf{S}}_{j,2,z} - \frac{1}{4}\hat{n}_{j,1,z}\hat{n}_{j,2,z}\right) - 2J_{\mathrm{H}}\sum_{j,l}\left(\hat{\mathbf{S}}_{j,l,x}\cdot\hat{\mathbf{S}}_{j,l,z} + \frac{1}{4}\hat{n}_{j,l,x}\hat{n}_{j,l,z}\right). \quad (2)$$

$\hat{\tilde{c}}_{j,l,\mu,\sigma} = \hat{c}_{j,l,\mu,\sigma}(1 - \hat{n}_{j,l,\mu,\bar{\sigma}})$ is the projected annihilation operator of $\hat{c}_{j,l,\mu,\sigma}$ for an electron with spin $\sigma$ $(=\uparrow,\downarrow)$ at site $j$ in chain $l$ $(=1,2)$, and orbital $\mu$ $(=x,z)$, where $\hat{n}_{j,l,\mu,\sigma} = \hat{c}^{\dagger}_{j,l,\mu,\sigma}\hat{c}_{j,l,\mu,\sigma}$ $(\hat{n}_{j,l,\mu} = \sum_\sigma \hat{n}_{j,l,\mu,\sigma})$ is the number operator and $\bar{\sigma}$ indicates the opposite spin of $\sigma$. Considering the bilayer nickelate system within a one-dimensional effective model, the orbitals $x$ and $z$ are associated with the $d_{x^2-y^2}$ and $d_{3z^3-r^2}$ orbitals, respectively. $\hat{\mathbf{S}}_{j,l,\mu} = (1/2)\sum_{\sigma,\sigma'}\hat{c}^{\dagger}_{j,l,\mu,\sigma}\boldsymbol{\sigma}_{\sigma,\sigma'}\hat{c}_{j,l,\mu,\sigma'}$ is the spin operator at site $j$ in chain $l$, and orbital $\mu$, where $\boldsymbol{\sigma}$ is a set of Pauli matrices $\boldsymbol{\sigma} = (\sigma^1, \sigma^2, \sigma^3)$. $\Delta E$ $(>0)$ is the energy difference between two orbitals, where the energy of the $x$ orbital is higher than the energy of the $z$ orbital, i.e., the $z$ $(x)$ orbital becomes nearly half (quarter) filling. $t_{\parallel}^{\mu\nu}$ and $t_{\perp}^{\mu\nu}$ denote the intrachain and interchain hoppings, respectively. $J_{\parallel}^{\mu\nu}$ and $J_{\perp}^{\mu\nu}$ indicate the intrachain and interchain spin-exchange couplings, respectively, and $J_{\mathrm{H}}$ $(>0)$ is the Hund's (interorbital ferromagnetic) coupling.

As for the interchain hopping $t_{\perp}^{\mu\nu}$, assuming that the overlap between two $d_{x^2-y^2}$ orbitals along the $z$ (rung) direction is small enough, we consider only interchain hopping $t_{\perp}^{zz}$ for the $d_{3z^2-r^2}$ orbital. In the high-symmetry structure (without tilt) of the bilayer nickelate under pressure, the interlayer hopping between the $d_{x^2-y^2}$ and $d_{3z^2-r^2}$ orbitals is zero, justifying $t_{\perp}^{xz} = 0$. On the other hand, we take into account all intrachain hoppings. In this paper, we set $t_{\parallel}^{xx} = 1$ as the energy unit and assume $t_{\parallel}^{zz} = 0.25$ and $t_{\parallel}^{xz} = 0.5$ to make a correspondence to the ratios of the intralayer hoppings estimated by the first-principle calculation in $La_3Ni_2O_7$ [39]. We use $t_{\perp}^{zz} = 0.7$ and $\Delta E = 1$ employed in Ref. [40] that suggests a good signature for superconductivity in the two-orbital Hubbard model. The results with different values of $t_{\perp}^{zz}$ and $\Delta E$ are presented in the Supplemental Material [60].

As for the spin interactions, we consider the intrachain antiferromagnetic coupling for the $x$ orbital $J_{\parallel}^{xx}$ $(>0)$ and interchain antiferromagnetic coupling for the $z$ orbital $J_{\perp}^{zz}$ $(>0)$. Since $J_{\parallel}^{zz}$ and $J_{\parallel}^{xz}$ are small relative to $J_{\parallel}^{xx}$ and $J_{\perp}^{zz}$ in the bilayer nickelate, we neglect $J_{\parallel}^{zz}$ and $J_{\parallel}^{xz}$ for simplicity. To comprehensively investigate the roles of the essential spin interactions in pairing properties within the two-orbital ladder model, we set $J_{\perp}^{zz}$ and $J_{\mathrm{H}}$ as variables while keeping $J_{\parallel}^{xx} = 0.5$. Assuming that the antiferromagnetic $J$ is on the order of $4t^2/U$ (where $U$ is the Hubbard repulsion), we have $J_{\parallel}^{xx} \simeq 0.5$ and $J_{\perp}^{zz} \simeq 0.25$ for $U = 8$ with $t_{\parallel}^{xx}$ as the energy unit. The ratio $J_{\perp}^{zz}/J_{\parallel}^{xx}$, however, could vary from two due to unaccounted factors in the aforementioned estimation such as the interorbital repulsion $U'$ and the ligand $p$ orbital between the nickel ions.

As shown in Fig. 1, the $z$ orbitals form the nearly half-filled ladder consisting of the strong interchain coupling ($t_{\perp}^{zz}$ and $J_{\perp}^{zz}$) and weak intrachain coupling ($t_{\parallel}^{zz}$). The electrons in the $x$ orbitals, which do not possess interchain couplings, are originally itinerant along the chain direction, while the interorbital hopping $t_{\parallel}^{xz}$ hybridizes the $x$ and $z$ networks. In addition, Hund's coupling $J_{\mathrm{H}}$ aligns the spins in the $x$ and $z$ orbitals within the single ion.

To compute the ground state of the two-orbital $t$-$J$ ladder, we employ the DMRG method implemented in the ITensor library [61]. We carry out the DMRG calculations in ladders of lengths $L = 48$ $(2 \times 48$ sites) with open boundary conditions. In this paper, we show the results at the bond dimension $m = 10\,000$, where the truncation errors are on the order of at most $10^{-6}$. We examine the $m$ and $L$ dependence of the results in the Supplemental Material [60]. As shown in Fig. 2, the $z$ $(x)$ orbital is nearly half (quarter) filling in the ground state. Electron filling of each orbital is not significantly changed by Hund's coupling $J_{\mathrm{H}}$. While $n_x(j)$ exhibits an oscillation when $J_{\mathrm{H}} = 1$, the oscillations are small around the center of the ladder and a charge-density-wave character is not substantial. To explore the nature of superconductivity in the two-orbital $t$-$J$ ladder, we calculate

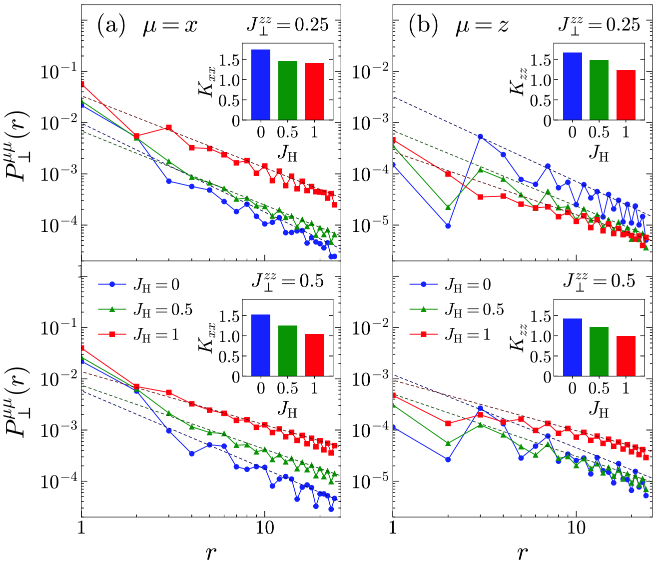


FIG. 3. Pair correlation functions $P_{\perp}^{\mu\mu}(r)$ for various values of Hund's coupling $J_{\rm H}$. (a) $P_{\perp}^{xx}(r)$ at $J_{\perp}^{zz} = 0.25$ (upper panel) and $J_{\perp}^{zz} = 0.5$ (lower panel). (b) $P_{\perp}^{zz}(r)$ at $J_{\perp}^{zz} = 0.25$ (upper panel) and $J_{\perp}^{zz} = 0.5$ (lower panel). The insets show the decay exponents of $P_{\perp}^{\mu\mu}(r)$, where the exponent $K_{\mu\mu}$ is extracted by fitting the crests of the data points at $r \geqslant 6$.

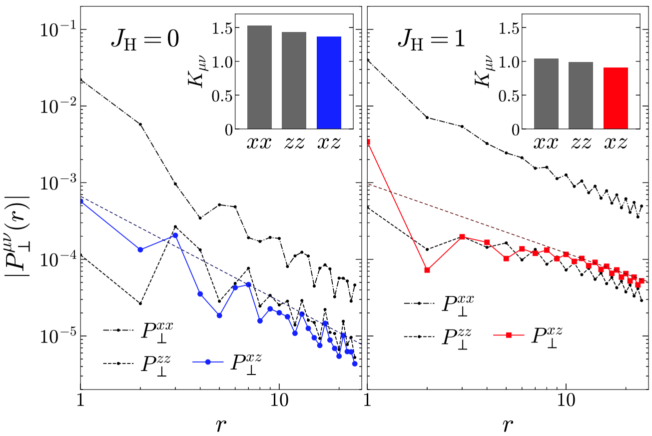


FIG. 4. Interorbital pair correlation functions $P_{\perp}^{xz}(r)$ at $J_{\rm H} = 0$ (left panel) and $J_{\rm H} = 1$ (right panel), where $J_{\perp}^{zz} = 0.5$. Intraorbital pair correlation functions $P_{\perp}^{\mu\mu}(r)$ are also presented for comparison. The insets show the decay exponents of $P_{\perp}^{xz}(r)$ denoted by $K_{xz}$ with $K_{xx}$ and $K_{zz}$. The exponent $K_{xz}$ is extracted by fitting the crests of the data points at $r \geqslant 6$.

the pair correlation function $P_{\perp}^{\mu\mu}(r) = \langle \hat{\Delta}_{j,\mu\mu}^{\dagger} \hat{\Delta}_{j+r,\mu\mu} \rangle$, where $\hat{\Delta}_{j,\mu\mu} = (\hat{\tilde{c}}_{j,1,\mu,\uparrow}\hat{\tilde{c}}_{j,2,\mu,\downarrow} - \hat{\tilde{c}}_{j,1,\mu,\downarrow}\hat{\tilde{c}}_{j,2,\mu,\uparrow})/\sqrt{2}$ is the interchain spin-singlet pair annihilation operator on orbital $\mu$ (= $x, z$) at site $j$. Here, we show the pair correlation function for the reference site $j = j_{\rm ref} = L/4$.

In Fig. 3, we compare the pair correlation functions $P_{\perp}^{\mu\mu}(r)$ for various values of $J_{\perp}^{zz}$ and $J_{\rm H}$. We find that the pair correlations of both orbitals exhibit power-law decays ($P_{\perp}^{\mu\mu}(r) \propto r^{-K_{\mu\mu}}$), as is consistent with the behavior in the two-orbital Hubbard ladder [40]. Reflecting the presence of many carriers in the $x$ orbitals close to quarter filling $P_{\perp}^{xx}(r)$ is larger than $P_{\perp}^{zz}(r)$ in the range we plotted. In one-dimensional systems, on the other hand, the correlations persisting over long distances are also crucial, and therefore we show the decay exponent $K_{\mu\mu}$ in the inset of Fig. 3. Here, a smaller $K_{\mu\mu}$ is preferable to a quasi-long-range order (i.e., slower decay of the pair correlation). As seen in Fig. 3(b), the decay of $P_{\perp}^{zz}(r)$ at $J_{\perp}^{zz} = 0.5$ is slower (i.e., has smaller $K_{zz}$) than that at $J_{\perp}^{zz} = 0.25$. This tendency is consistent with the case in the one-orbital $t$-$J$ ladder, in which a larger $J_{\perp}$ is favorable for the pair formation [54,55]. Moreover, our calculations in the two-orbital $t$-$J$ ladder show that Hund's coupling $J_{\rm H}$ enhances the pair correlations at long distances, supporting a smaller decay exponent $K_{zz}$. $P_{\perp}^{xx}(r)$ in Fig. 3(a) also shows a similar decay tendency against $J_{\perp}^{zz}$ and $J_{\rm H}$. As summarized in the insets of Fig. 3, we find that larger $J_{\rm H}$ as well as larger $J_{\perp}^{zz}$ makes $K_{\mu\mu}$ smaller for both orbitals, i.e., they promote the quasi-long-range superconducting order. Arbitrariness in the choice of data points used for fitting and the choice of the reference site may affect the results for $K_{\mu\mu}$. We confirm that the $J_{\perp}^{zz}$ and $J_{\rm H}$ dependence of $K_{\mu\mu}$ gives a similar tendency to Fig. 3 even when different fitting procedures or averaged pair correlations are used (see the Supplemental Material [60]). While $K_{xx} > K_{zz}$ in most of the parameter sets used in Fig. 3, $K_{xx}$ is comparable to $K_{zz}$, suggesting that both orbitals cooperatively contribute to the pairing.

Curiously, $P_{\perp}^{xx}(r)$ exhibits a comparable power-law decay with $P_{\perp}^{zz}(r)$ even at $J_{\rm H} = 0$ (and $J_{\perp}^{xx} = 0$). This indicates that the orbital hybridization via $t_{\parallel}^{xz}$ is a crucial factor for the pair correlation of the $x$ component at $J_{\rm H} = 0$ because the interorbital coupling $J_{\rm H}$ (= 0) does not create the local interchain spin correlation between the $x$ orbitals, as we shall see explicitly later. A developed $x$-component pair correlation without $J_{\rm H}$ is also seen in the two-orbital Hubbard ladder [40]. The present result is even more curious than in the case of the Hubbard ladder because the intrachain-interorbital exchange coupling $J_{\parallel}^{xz}$, which is proportional to $\sim(t_{\parallel}^{xz})^2/U$ in the Hubbard ladder (at $U \gg \Delta E, t_{\parallel}^{xz}$) and can induce the interchain $x$-$x$ spin correlation through $z$-$z$ spin correlation, is absent in the present model. Here, to examine the interorbital contribution to the pairing more directly, we compute the correlation of the interchain-interorbital spin singlet pair described by $\hat{\Delta}_{j,xz} = (\hat{\tilde{c}}_{j,1,x,\uparrow}\hat{\tilde{c}}_{j,2,z,\downarrow} - \hat{\tilde{c}}_{j,1,x,\downarrow}\hat{\tilde{c}}_{j,2,z,\uparrow})/\sqrt{2}$ and present its correlation function $P_{\perp}^{xz}(r)$ in Fig. 4. The decay of $P_{\perp}^{xz}(r)$ is comparable to that of $P_{\perp}^{xx}(r)$ and $P_{\perp}^{zz}(r)$ at $J_{\rm H} = 0$, suggesting that the $x$-$z$ singlet pair also strongly contributes to the superconducting correlation. The decay exponent $K_{xz}$ is presented in the inset of Fig. 4, where $K_{xz}$ is the smallest and comparable to $K_{xx}$ and $K_{zz}$. Even if we extract $K_{\mu\nu}$ from the averaged pair correlation $\bar{P}_{\perp}^{\mu\nu}(r)$, we find a small decay exponent for the $x$-$z$ pair (see the Supplemental Material [60]). Our numerical demonstration implies that the interorbital component is also a considerable ingredient for the pairing in the presence of $t_{\parallel}^{xz}$. A slow decay of $P_{\perp}^{xz}(r)$ also appears at $J_{\rm H} = 1$ and the decay exponent $K_{xz}$ is still the smallest, suggesting the significance of the $x$-$z$ component of the pair regardless of $J_{\rm H}$.

To understand the underlying spin structure, we present the local interchain spin correlation $F_{\perp}^{\mu\nu}(j) = \langle \hat{\mathbf{S}}_{j,1,\mu} \cdot \hat{\mathbf{S}}_{j,2,\nu} \rangle$ and its average $\bar{F}_{\perp}^{\mu\nu}$ in Fig. 5. At $J_{\rm H} = 0$, $F_{\perp}^{zz}(j)$ is close to the value of the ideal spin-singlet (= $-0.75$) because of $J_{\perp}^{zz}$ that directly forms the spin-singlet, whereas $F_{\perp}^{xx}(j)$ and

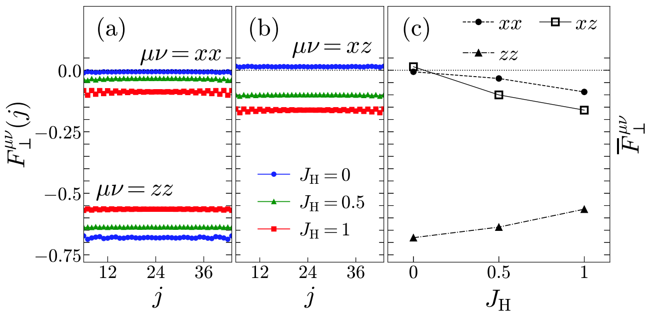


FIG. 5. Interchain spin correlation functions $F_\perp^{\mu\nu}(j) = \langle \hat{\boldsymbol{S}}_{j,1,\mu} \cdot \hat{\boldsymbol{S}}_{j,2,\nu} \rangle$ for various values of Hund's coupling $J_{\rm H}$ (where $J_\perp^{zz} = 0.5$). (a) Intraorbital components $F_\perp^{xx}(j)$ and $F_\perp^{zz}(j)$. (b) Interorbital component $F_\perp^{xz}(j)$. (c) $J_{\rm H}$ dependence of the averaged spin correlation $\bar{F}_\perp^{\mu\nu}$, where $F_\perp^{\mu\nu}(j)$ is averaged over the sites from $j = 12$ to $j = 36$.

$F_\perp^{xz}(j)$ are nearly zero reflecting $J_\perp^{xx} = J_\perp^{xz} = 0$. At large $J_{\rm H}$, on the other hand, antiferromagnetic correlations in $F_\perp^{xx}(j)$ and $F_\perp^{xz}(j)$ are enhanced by $J_{\rm H}$, implying that the effective $x$-$x$ and $x$-$z$ spin couplings are generated by the combination of $J_\perp^{zz}$ and $J_{\rm H}$ as pointed out by the previous studies [19,21]. While the $z$-$z$ component is suppressed by $J_{\rm H}$, its magnitude is still the largest. Hence, the glue of the $z$-$z$ pair is active even at larger $J_{\rm H}$.

The enhancement of the interchain $x$-$x$ and $x$-$z$ spin-singlet correlations ($F_\perp^{xx}$ and $F_\perp^{xz}$) upon increasing $J_{\rm H}$ is consistent with the enhancement of the $x$-$x$ and $x$-$z$ pair correlations ($P_\perp^{xx}$ and $P_\perp^{xz}$) seen in Figs. 3 and 4 as $J_{\rm H}$ is increased. On the other hand, there are some contrasting features between the interchain spin correlations and pair correlations. First, at $J_{\rm H} = 0$, both $x$-$z$ and $x$-$x$ spin correlations are very small, which is naturally expected in the absence of $J_\perp^{xx}$, $J_\perp^{xz}$, and $J_\parallel^{xz}$. This is in striking contrast to the fact that even at $J_{\rm H} = 0$, the interchain $x$-$z$ and $x$-$x$ pair correlations exhibit a slow decay. In other words, quasi-long-range interchain pair correlation develops in the $x$-$z$ and $x$-$x$ channel even in the absence of pairing glues mediated by $J_\perp^{zz}$ and $J_{\rm H}$ [19,21]. This suggests that in the presence of $t_\parallel^{xz}$, the pairs must be described by $x$-$z$ hybridized entities, where the pairing glue fundamentally originates from the strong interchain exchange coupling $J_\perp^{zz}$ of the nearly half-filled $z$ orbitals, but $x$-$z$ and $x$-$x$ interchain pair correlations are also comparably strong. Second, although $J_{\rm H}$ reduces the spin-singlet correlation of the $z$-$z$ component [see Fig. 5], $J_{\rm H}$ enhances the pair correlation $P_\perp^{zz}(r)$ [see Fig. 3]. This may also support our picture that the pairs should be described by $x$-$z$ hybridized entities in the presence of $t_\parallel^{xz}$. Namely, the enhancement of the $x$-$z$ pair correlation with increased $J_{\rm H}$ results in an enhanced pair correlation of the $x$-$z$ hybridized entity as a whole, and hence leads to the enhancement of the $z$-$z$ pair correlation.

Since the hybridization due to $t_\parallel^{xz}$ gives the nonlocal effects, an interpretation of the pair in real space is nontrivial. The optimal definition of the local pair and examination of its pair correlation in strongly correlated and hybridized two-orbital systems is an important open issue. We must also note that the hybridization effect in one-dimensional systems is strong relative to the actual two-dimensional $La_3Ni_2O_7$, in which the hybridization between the $d_{x^2-y^2}$ and $d_{3z^2-r^2}$ orbitals vanishes along the $k_x = \pm k_y$ line on the square lattice [1]. Hence, our idea for the ladder system may potentially overestimate the effect of $t_\parallel^{xz}$ in the actual two-dimensional bilayer nickelate. Also, we considered only Hund's coupling $J_{\rm H}$ as the interorbital two-body interaction. The effect of other interorbital interactions such as the interorbital repulsion $U'$ or the pair hopping $J_{\rm pair}$ remains an open issue. In fact, if we apply the fluctuation exchange approximation, which is basically a weak coupling approach, to a three-dimensional model of $La_3Ni_2O_7$, we find that while $J_{\rm H}$ alone does enhance superconductivity within a realistic parameter range, both $U'$ and $J_{\rm pair}$ suppress superconductivity [62] so that the two-body interorbital interactions in total result in a slight suppression of superconductivity [39].

To summarize, we have investigated the pair correlations using DMRG in a two-orbital $t$-$J$ ladder including Hund's coupling that mimics $La_3Ni_2O_7$. Our calculation demonstrates that the correlation of the interorbital $x$-$z$ pairs exhibits a slow power-law decay as well as the $x$-$x$ and $z$-$z$ pairs, and they are promoted by Hund's coupling $J_{\rm H}$. Our numerics suggest that the hybridized entity due to the interorbital hopping $t_\parallel^{xz}$ obtains the quasi-long-range superconducting correlation. The necessity of such a picture for describing the pairing state in the two-orbital ladder system may have some implications on the superconductivity in the bilayer nickelate.

*Note added.* Recently, we became aware of another theoretical study that performs DMRG calculations in a $t$-$J$ model [45] during the finalization process of the present study. The model studied there is similar to ours, and the tendency of the pair correlation against Hund's coupling is consistent while the different parameter regimes are studied. Besides, we studied the interorbital pair correlations, which were not studied in this, or any other previous studies.

This work was supported by Grants-in-Aid for Scientific Research from JSPS, KAKENHI Grants No. JP20H01849, No. JP24K06939 (T.K.), No. JP22K03512 (H.S.), No. JP22K04907, (K.K.), and No. JP24K01333. M.K. was supported by Program for Leading Graduate Schools: Interactive Materials Science Cadet Program and by Kato Foundation for Promotion of Science, Grant No. KS-3614. The computing resource is supported by the supercomputer system (system-B) in the Institute for Solid State Physics, the University of Tokyo, and the supercomputer of Academic Center for Computing and Media Studies (ACCMS), Kyoto University. The DMRG calculations were performed using the ITensor library [61].

[1] H. Sun, M. Huo, X. Hu, J. Li, Z. Liu, Y. Han, L. Tang, Z. Mao, P. Yang, B. Wang, J. Cheng, D.-X. Yao, G.-M. Zhang, and M. Wang, Signatures of superconductivity near 80 K in a nickelate under high pressure, Nature (London) **621**, 493 (2023).

[2] J. Hou, P. T. Yang, Z. Y. Liu, J. Y. Li, P. F. Shan, L. Ma, G. Wang, N. N. Wang, H. Z. Guo, J. P. Sun, Y. Uwatoko, M. Wang, G.-M. Zhang, B. S. Wang, and J.-G. Cheng, Emergence of high-temperature superconducting phase in the pressurized $La_3Ni_2O_7$ crystals, Chin. Phys. Lett. **40**, 117302 (2023).

[3] Y. Zhang, D. Su, Y. Huang, H. Sun, M. Huo, Z. Shan, K. Ye, Z. Yang, R. Li, M. Smidman, M. Wang, L. Jiao, and H. Yuan, High-temperature superconductivity with zero-resistance and strange metal behavior in $La_3Ni_2O_7$, arXiv:2307.14819.

[4] G. Wang, N. N. Wang, X. L. Shen, J. Hou, L. Ma, L. F. Shi, Z. A. Ren, Y. D. Gu, H. M. Ma, P. T. Yang, Z. Y. Liu, H. Z. Guo, J. P. Sun, G. M. Zhang, S. Calder, J.-Q. Yan, B. S. Wang, Y. Uwatoko, and J.-G. Cheng, Pressure-induced superconductivity in polycrystalline $La_3Ni_2O_{7-\delta}$, Phys. Rev. X **14**, 011040 (2024).

[5] H. Sakakibara, M. Ochi, H. Nagata, Y. Ueki, H. Sakurai, R. Matsumoto, K. Terashima, K. Hirose, H. Ohta, M. Kato, Y. Takano, and K. Kuroki, Theoretical analysis on the possibility of superconductivity in a trilayer Ruddlesden-Popper nickelate $La_4Ni_3O_{10}$ under pressure and its experimental examination: Comparison with $La_3Ni_2O_7$, Phys. Rev. B **109**, 144511 (2024).

[6] G. Wang, N. Wang, Y. Yuxin Wang, L. Shi, X. Shen, J. Hou, H. Ma, P. Yang, Z. Liu, H. Zhang, X. Dong, J. Sun, B. Wang, K. Jiang, J. Hu, Y. Uwatoko, and J. Cheng, Observation of high-temperature superconductivity in the high-pressure tetragonal phase of $La_2PrNi_2O_{7-\delta}$, arXiv:2311.08212.

[7] Y. Zhou, J. Guo, S. Cai, H. Sun, P. Wang, J. Zhao, J. Han, X. Chen, Q. Wu, Y. Ding, M. Wang, T. Xiang, H.-K. Mao, and L. Sun, Evidence of filamentary superconductivity in pressurized $La_3Ni_2O_{7-\delta}$ single crystals, arXiv:2311.12361.

[8] Z. Luo, X. Hu, M. Wang, W. Wú, and D.-X. Yao, Bilayer two-orbital model of $La_3Ni_2O_7$ under pressure, Phys. Rev. Lett. **131**, 126001 (2023).

[9] Q.-G. Yang, D. Wang, and Q.-H. Wang, Possible $s_\pm$-wave superconductivity in $La_3Ni_2O_7$, Phys. Rev. B **108**, L140505 (2023).

[10] V. Christiansson, F. Petocchi, and P. Werner, Correlated electronic structure of $La_3Ni_2O_7$ under pressure, Phys. Rev. Lett. **131**, 206501 (2023).

[11] Y.-F. Yang, G.-M. Zhang, and F.-C. Zhang, Interlayer valence bonds and two-component theory for high-$T_c$ superconductivity of $La_3Ni_2O_7$ under pressure, Phys. Rev. B **108**, L201108 (2023).

[12] Y. Zhang, L.-F. Lin, A. Moreo, T. A. Maier, and E. Dagotto, Trends in electronic structures and $s_\pm$-wave pairing for the rare-earth series in bilayer nickelate superconductor $R_3Ni_2O_7$, Phys. Rev. B **108**, 165141 (2023).

[13] Y. Zhang, L.-F. Lin, A. Moreo, and E. Dagotto, Electronic structure, dimer physics, orbital-selective behavior, and magnetic tendencies in the bilayer nickelate superconductor $La_3Ni_2O_7$ under pressure, Phys. Rev. B **108**, L180510 (2023).

[14] F. Lechermann, J. Gondolf, S. Bötzel, and I. M. Eremin, Electronic correlations and superconducting instability in $La_3Ni_2O_7$ under high pressure, Phys. Rev. B **108**, L201121 (2023).

[15] W. Wú, Z. Luo, D.-X. Yao, and M. Wang, Superexchange and charge transfer in the nickelate superconductor $La_3Ni_2O_7$ under pressure, Sci. China Phys. Mech. Astron. **67**, 117402 (2024).

[16] Y. Cao and Y.-F. Yang, Flat bands promoted by Hund's rule coupling in the candidate double-layer high-temperature superconductor $La_3Ni_2O_7$ under high pressure, Phys. Rev. B **109**, L081105 (2024).

[17] X. Chen, P. Jiang, J. Li, Z. Zhong, and Y. Lu, Critical charge and spin instabilities in superconducting $La_3Ni_2O_7$, arXiv:2307.07154.

[18] Y.-B. Liu, J.-W. Mei, F. Ye, W.-Q. Chen, and F. Yang, $s^\pm$-wave pairing and the destructive role of apical-oxygen deficiencies in $La_3Ni_2O_7$ under pressure, Phys. Rev. Lett. **131**, 236002 (2023).

[19] C. Lu, Z. Pan, F. Yang, and C. Wu, Interlayer-coupling-driven high-temperature superconductivity in $La_3Ni_2O_7$ under pressure, Phys. Rev. Lett. **132**, 146002 (2024).

[20] Y. Zhang, L.-F. Lin, A. Moreo, T. A. Maier, and E. Dagotto, Structural phase transition, $s_\pm$-wave pairing, and magnetic stripe order in bilayered superconductor $La_3Ni_2O_7$ under pressure, Nat. Commun. **15**, 2470 (2024).

[21] H. Oh and Y.-H. Zhang, Type-II $t-J$ model and shared superexchange coupling from Hund's rule in superconducting $La_3Ni_2O_7$, Phys. Rev. B **108**, 174511 (2023).

[22] Z. Liao, L. Chen, G. Duan, Y. Wang, C. Liu, R. Yu, and Q. Si, Electron correlations and superconductivity in $La_3Ni_2O_7$ under pressure tuning, Phys. Rev. B **108**, 214522 (2023).

[23] K. Jiang, Z. Wang, and F.-C. Zhang, High-temperature superconductivity in $La_3Ni_2O_7$, Chin. Phys. Lett. **41**, 017402 (2024).

[24] Q. Qin and Y.-F. Yang, High-$T_c$ superconductivity by mobilizing local spin singlets and possible route to higher $T_c$ in pressurized $La_3Ni_2O_7$, Phys. Rev. B **108**, L140504 (2023).

[25] Y.-H. Tian, Y. Chen, J.-M. Wang, R.-Q. He, and Z.-Y. Lu, Correlation effects and concomitant two-orbital $s_\pm$-wave superconductivity in $La_3Ni_2O_7$ under high pressure, Phys. Rev. B **109**, 165154 (2024).

[26] D.-C. Lu, M. Li, Z.-Y. Zeng, W. Hou, J. Wang, F. Yang, and Y.-Z. You, Superconductivity from doping symmetric mass generation insulators: Application to $La_3Ni_2O_7$ under pressure, arXiv:2308.11195.

[27] R. Jiang, J. Hou, Z. Fan, Z.-J. Lang, and W. Ku, Pressure driven fractionalization of ionic spins results in cupratelike high-$T_c$ superconductivity in $La_3Ni_2O_7$, Phys. Rev. Lett. **132**, 126503 (2024).

[28] Z. Luo, B. Lv, M. Wang, W. Wú, and D.-X. Yao, High-$T_C$ superconductivity in $La_3Ni_2O_7$ based on the bilayer two-orbital t-J model, arXiv:2308.16564.

[29] J.-X. Zhang, H.-K. Zhang, Y.-Z. You, and Z.-Y. Weng, Strong pairing originated from an emergent $\mathbb{Z}_2$ berry phase in $La_3Ni_2O_7$, arXiv:2309.05726.

[30] B. Geisler, J. J. Hamlin, G. R. Stewart, R. G. Hennig, and P. J. Hirschfeld, Structural transitions, octahedral rotations, and electronic properties of $A_3Ni_2O_7$ rare-earth nickelates under high pressure, npj Quantum Mater. **9**, 38 (2024).

[31] C. Lu, Z. Pan, F. Yang, and C. Wu, Interplay of two $E_g$ orbitals in superconducting $La_3Ni_2O_7$ under pressure, arXiv:2310.02915.

[32] Y. Gu, C. Le, Z. Yang, X. Wu, and J. Hu, Effective model and pairing tendency in bilayer Ni-based superconductor $La_3Ni_2O_7$, arXiv:2306.07275.

[33] Y. Zhang, L.-F. Lin, A. Moreo, T. A. Maier, and E. Dagotto, Electronic structure, magnetic correlations, and superconducting pairing in the reduced Ruddlesden-Popper bilayer $La_3Ni_2O_6$ under pressure: Different role of $d_{3z^2-r^2}$ orbital compared with $La_3Ni_2O_7$, Phys. Rev. B **109**, 045151 (2024).

[34] U. Kumar, C. Melnick, and G. Kotliar, Softening of $dd$ excitation in the resonant inelastic x-ray scattering spectra as a signature of Hund's coupling in nickelates, arXiv:2310.00983.

[35] Z. Ouyang, J.-M. Wang, J.-X. Wang, R.-Q. He, L. Huang, and Z.-Y. Lu, Hund electronic correlation in $La_3Ni_2O_7$ under high pressure, Phys. Rev. B **109**, 115114 (2024).

[36] H. Liu, C. Xia, S. Zhou, and H. Chen, Role of crystal-field-splitting and longe-range-hoppings on superconducting pairing symmetry of $La_3Ni_2O_7$, arXiv:2311.07316.

[37] S. Ryee, N. Witt, and T. O. Wehling, Quenched pair breaking by interlayer correlations as a key to superconductivity in $La_3Ni_2O_7$, arXiv:2310.17465.

[38] J. Chen, F. Yang, and W. Li, Orbital-selective superconductivity in the pressurized bilayer nickelate $La_3Ni_2O_7$: An infinite projected entangled-pair state study, arXiv:2311.05491.

[39] H. Sakakibara, N. Kitamine, M. Ochi, and K. Kuroki, Possible high $T_c$ superconductivity in $La_3Ni_2O_7$ under high pressure through manifestation of a nearly half-filled bilayer Hubbard model, Phys. Rev. Lett. **132**, 106002 (2024).

[40] T. Kaneko, H. Sakakibara, M. Ochi, and K. Kuroki, Pair correlations in the two-orbital Hubbard ladder: Implications for superconductivity in the bilayer nickelate $La_3Ni_2O_7$, Phys. Rev. B **109**, 045154 (2024).

[41] Y. Shen, M. Qin, and G.-M. Zhang, Effective Bi-Layer model Hamiltonian and density-matrix renormalization group study for the high-$T_c$ superconductivity in $La_3Ni_2O_7$ under high pressure, Chin. Phys. Lett. **40**, 127401 (2023).

[42] X.-Z. Qu, D.-W. Qu, J. Chen, C. Wu, F. Yang, W. Li, and G. Su, Bilayer $t$-$J$-$J_\perp$ model and magnetically mediated pairing in the pressurized nickelate $La_3Ni_2O_7$, Phys. Rev. Lett. **132**, 036502 (2024).

[43] H. Lange, L. Homeier, E. Demler, U. Schollwöck, F. Grusdt, and A. Bohrdt, Feshbach resonance in a strongly repulsive ladder of mixed dimensionality: A possible scenario for bilayer nickelate superconductors, Phys. Rev. B **109**, 045127 (2024).

[44] H. Schlömer, U. Schollwöck, F. Grusdt, and A. Bohrdt, Superconductivity in the pressurized nickelate $La_3Ni_2O_7$ in the vicinity of a BEC-BCS crossover, arXiv:2311.03349.

[45] X.-Z. Qu, D.-W. Qu, W. Li, and G. Su, Roles of Hund's rule and hybridization in the two-orbital model for high-$t_c$ superconductivity in the bilayer nickelate, arXiv:2311.12769.

[46] Q. Li, Y.-J. Zhang, Z.-N. Xiang, Y. Zhang, X. Zhu, and H.-H. Wen, Signature of superconductivity in pressurized $La_4Ni_3O_{10}$, Chin. Phys. Lett. **41**, 017401 (2024).

[47] Y. Zhu, E. Zhang, B. Pan, X. Chen, D. Peng, L. Chen, H. Ren, F. Liu, N. Li, Z. Xing, J. Han, J. Wang, D. Jia, H. Wo, Y. Gu, Y. Gu, L. Ji, W. Wang, H. Gou, Y. Shen, T. Ying, X. Chen, W. Yang, C. Zheng, Q. Zeng, J. gang Guo, and J. Zhao, Superconductivity in trilayer nickelate $La_4Ni_3O_{10}$ single crystals, arXiv:2311.07353.

[48] M. Zhang, C. Pei, X. Du, W. Hu, Y. Cao, Q. Wang, J. Wu, Y. Li, H. Liu, C. Wen, Y. Zhao, C. Li, W. Cao, S. Zhu, Q. Zhang, N. Yu, P. Cheng, L. Zhang, Z. Li, J. Zhao, Y. Chen, H. Guo, C. Wu, F. Yang, S. Yan, L. Yang, and Y. Qi, Superconductivity in trilayer nickelate $La_4Ni_3O_{10}$ under pressure, arXiv:2311.07423.

[49] M. Nakata, D. Ogura, H. Usui, and K. Kuroki, Finite-energy spin fluctuations as a pairing glue in systems with coexisting electron and hole bands, Phys. Rev. B **95**, 214509 (2017).

[50] K. Kuroki, T. Kimura, and R. Arita, High-temperature superconductivity in dimer array systems, Phys. Rev. B **66**, 184508 (2002).

[51] T. A. Maier and D. J. Scalapino, Pair structure and the pairing interaction in a bilayer Hubbard model for unconventional superconductivity, Phys. Rev. B **84**, 180513(R) (2011).

[52] V. Mishra, D. J. Scalapino, and T. A. Maier, $s_\pm$ pairing near a Lifshitz transition, Sci. Rep. **6**, 32078 (2016).

[53] T. A. Maier, V. Mishra, G. Balduzzi, and D. J. Scalapino, Effective pairing interaction in a system with an incipient band, Phys. Rev. B **99**, 140504(R) (2019).

[54] E. Dagotto, J. Riera, and D. Scalapino, Superconductivity in ladders and coupled planes, Phys. Rev. B **45**, 5744(R) (1992).

[55] M. Troyer, H. Tsunetsugu, and T. M. Rice, Properties of lightly doped $t$-$J$ two-leg ladders, Phys. Rev. B **53**, 251 (1996).

[56] M. Dolfi, B. Bauer, S. Keller, and M. Troyer, Pair correlations in doped Hubbard ladders, Phys. Rev. B **92**, 195139 (2015).

[57] S. R. White, Density matrix formulation for quantum renormalization groups, Phys. Rev. Lett. **69**, 2863 (1992).

[58] S. R. White, Density-matrix algorithms for quantum renormalization groups, Phys. Rev. B **48**, 10345 (1993).

[59] U. Schollwöck, The density-matrix renormalization group in the age of matrix product states, Ann. Phys. **326**, 96 (2011).

[60] See Supplemental Material at http://link.aps.org/supplemental/10.1103/PhysRevB.109.L201124 for supplemental numerical results.

[61] M. Fishman, S. R. White, and E. M. Stoudenmire, The ITensor software library for tensor network calculations, SciPost Phys. Codebases, 4 (2022).

[62] H. Sakakibara, M. Ochi, and K. Kuroki (unpublished).